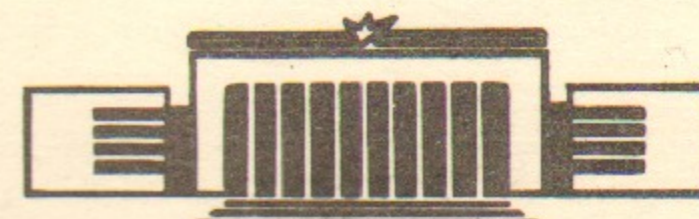ИНСТИТУТ ЯДЕРНОЙ ФИЗИКИ
СО АН СССР

Boris V. Chirikov

CHAOTIC DYNAMICS IN HAMILTONIAN SYSTEMS WITH DIVIDED PHASE SPACE

PREPRINT 82-132

Новосибирск

1. Introduction

The subject of this lecture is related to a peculiar dynamical phenomenon in classical mechanics commonly termed among physicists as the chaotic, or stochastic, motion. Until recently the mathematicians used to say just about ergodic properties of a dynamical system. However, nowadays the term "random motion" becomes also popular. I would like to emphasize from the beginning that the problem we are going to discuss is purely dynamical, without any random element either in the equations of motion or in initial conditions. Hence, the term - - dynamical, or intrinsic chaos. Below we restrict ourselves to only Hamiltonian dynamics for which the invariant measure (phase space volume) is known beforehand, unlike dissipative systems.

The interest to the dynamical chaos is twofold. First, it is a fundamental phenomenon in physics which, in particular, gives, at last, a long-awaited model for the true random process. Second, no matter how strange the random dynamics may appear it turns out to be fairly widespread in many fields of science and technology as, in particular, the present Conference demonstrates.

On a rare occasion, when chaos comprises all the phase space of a dynamical system or, at least, a whole invariant surface of the motion, a fairly simple statistical description is possible as contrasted to most complicated dynamical picture of motion.

In many cases, however, the situation is not that simple. A typical example is the so-called divided phase space, divided into the regions of both chaotic and regular motions separated by highly intricate borders. It is the structure of that chaos border which considerably complicates also the statistical description of the motion. Even though the mathematical theory of dynamical systems admits divided phase space and, moreover, does term it by a special notion - ergodic component - not much is actually known thus far on the dynamical behavior therein. Below we are going to consider a number of

selected questions related to this topic. I choose an old Po-
incaré problem, which is still not solved completely, to dis-
cuss some recent developments in this field.

A general review of the modern mathematical theory can be
found in [1-3], while related physical theory is surveyed, e.g.,
in [4,5].

2. Poincare's problem

We begin with a "simple" example considered by Poincare[6]
in his attempt to understand profound difficulties arising in
the study of nonlinear dynamics, in general, and of the famous
three body problem, in particular. Much later, this example has
proven to typify a fairly general situation in Hamiltonian dy-
namics (see [4] and Section 3b below).

Consider the motion of the ordinary pendulum under a high
frequency parametric perturbation as described by the Hamilto-
nian

$$H(p, \varphi, \theta) = \frac{p^2}{2} + \omega_o^2 \cdot \cos\varphi \cdot (1 + \varepsilon \cdot \cos\theta) \qquad (2.1)$$

Here φ is the angular position of pendulum ($\varphi = 0$ corres-
ponds to the unstable equilibrium); $p = \dot{\varphi}$ is angular momentum,
and ω_o is the frequency of small oscillation. The perturbati-
on is characterized by its strength $\varepsilon \ll 1$, and by the phase
θ ($\dot{\theta} = \Omega$). There are two small parameters in the problem
under consideration: i) the perturbation strength ε ; ii) the
adiabaticity parameter

$$\frac{1}{\lambda} = \frac{\omega_o}{\Omega} \ll 1 \qquad (2.2)$$

Traditionally, the adiabatic perturbation is assumed to be
low-frequency. Yet, it is only a half of the story. Since per-
turbation of a system is a part of its interaction with ano-
ther system (degree of freedom) the back perturbation would
be high-frequency, and vice versa.

The motion of the unperturbed ($\varepsilon = 0$) pendulum, as is
well known, is periodic for any initial conditions with one

4

important exception, corresponding to the value of $H = \omega_o^2$.
The latter trajectory is called separatrix since it separa-
tes the pendulum oscillation ($H < \omega_o^2$) from its rotation
($H > \omega_o^2$). In what follows the separatrix is going to play a
leading part in dynamical chaos.

The motion period T is increasing idenfinitely when ap-
proaching separatrix. In immediate vicinity of the latter

$$T \approx \frac{1}{\omega_o} \ln\frac{32}{|w|} ; \qquad w = \frac{H}{\omega_o^2} - 1 \qquad (2.3)$$

Note that for oscillation ($w < 0$) the quantity T is actually
a half-period. The separatrix motion is, thus, aperiodic, and
it has continuous Fourier spectrum which may be characterized
by the integral [4]:

$$A_m(\lambda) = \omega_o \int_{-\infty}^{\infty} e^{i\left(\frac{m}{2}\varphi_s(t) - \Omega t\right)} dt \approx \frac{4\pi}{\Gamma(m)} \cdot (2\lambda)^{m-1} \cdot e^{-\pi\lambda/2} \qquad (2.4)$$

The last expression holds for $\lambda \gg 1$; $\Gamma(m)$ is the gamma fun-
ction with any positive real m, and [6]

$$\varphi_s(t) = 4 \cdot \arctan\left(e^{\omega_o t}\right) - \pi \qquad (2.5)$$

is the separatrix motion (in case of $m < 0$ $A_m = A_{|m|} \cdot \exp(-\pi\lambda)$).

What is the impact of perturbation on the pendulum moti-
on? The first move would be to consider the perturbation as
completely nonresonant because of the condition $\lambda \gg 1$. Then,
in the first approximation of the asymptotic theory [7] the
perturbation can be neglected, or averaged out. Yet, in the
second approximation it changes the effective potential:

$$U(\varphi) = \omega_o^2 \cdot \cos\varphi \longrightarrow \omega_o^2 \cdot \left(\cos\varphi - \frac{\varepsilon^2}{8\lambda^2}\cos 2\varphi\right) \qquad (2.6)$$

This leads, in particular, to a shift of frequencies at both
stable and unstable equilibria:

$$\omega_{st}^2 = \omega_o^2 \longrightarrow \omega_o^2 \cdot \left(1 + \frac{\varepsilon^2}{2\lambda^2}\right)$$

$$\omega_{us}^2 = -\omega_o^2 \longrightarrow -\omega_o^2 \cdot \left(1 - \frac{\varepsilon^2}{2\lambda^2}\right) \qquad (2.7)$$

5

We shall use this result later on.

Now, let us inspect the perturbation more carefully. Is it really completely nonresonant? And is the change (2.6) its only effect? Certainly, it is not on the separatrix, as is obvious from the boundless spectrum (2.4). Hence, in some vicinity around separatrix we also cannot neglect the perturbation even in the first approximation.

That the motion here is very sensitive to perturbation, which makes it highly intricate, has been found out and well recognized already by Poincaré. He was very close to the discovery of chaotic dynamics although he did never use this sort of language, instead speaking just about homoclinic solutions, or trajectories. One of the problems he has left to future researchers was to find out the dimension, structure, and measure of the homoclinic region near separatrix.

3. Solution of the Poincaré problem

a. Separatrix mapping

First, we construct a mapping describing the motion near separatrix in finite time steps. It is natural to choose the motion period T as the time step. Then, the change in energy w over this step is given by the integral of the type (2.4) while the change in perturbation phase θ is determined by the dependence (2.3). Thus, we arrive at the mapping $(w, \theta \to \bar{w}, \bar{\theta})$ [4]:

$$\bar{w} = w + \xi \cdot \sin\theta; \qquad \bar{\theta} = \theta + \lambda \cdot \ln\frac{32}{|w|} \qquad (3.1)$$

which we shall call the separatrix mapping.

The new perturbation parameter ξ is given by the expression

$$\xi = -4\pi\varepsilon\lambda^2 e^{-\pi\lambda/2} \qquad (3.2)$$

While ξ is proportional to small parameter ε, it cannot be expanded in powers of adiabaticity parameter $1/\lambda$. Hence, as is commonly believed, the expression (3.2) as well as the map (3.1) go beyond the asymptotic perturbation theory. However,

one can argue in a different way: it is not so much a fault of asymptotic theory but, rather, our own failure to choose the proper, adequate perturbation parameter. In other words, the true small parameter of the adiabatic perturbation is not the usual one $1/\lambda$, which enters the original Hamiltonian, but another one which explicitly takes account of weak resonances present in spite of adiabatic conditions. An important point of this philosophy relates to the fact that there is no principal difficulty in evaluating this ξ. The evaluation actually follows the usual asymptotic procedure of successive approximations since the unperturbed separatrix motion (2.5) is used. The really crucial difference from earlier unsuccessful approaches to Poincaré's and similar problems lies in seeking out the resonances even if they do appear to be absent.

Parameter ξ immediately gives the so-called splitting of separatrix, i.e. a gap between the two branches of separatrix going up and down in time (the first corresponds to $w = 0$, and the second does so to $\bar{w} = 0$, the maximal gap being $2|\xi|$). This effect has been also discovered by Poincaré[6] (Section 401). In our time it was further studied by Melnikov[8], Shilnikov[9] and others.

Separatrix splitting is a very important dynamical phenomenon. Yet, it does not tell us anything about a long-term evolution of the system. Are variations of w restricted or unbounded?

Before to proceed further we transform (3.1) introducing a new variable $y = w/\xi$, that is we take half of separatrix splitting as the unit for w. Ignoring a constant phase shift in the second equation (3.1) (see Section 3c) we arrive at the reduced map

$$\bar{y} = y + \sin\theta; \qquad \bar{\theta} = \theta - \lambda \cdot \ln|\bar{y}| \qquad (3.3)$$

with the only parameter λ. In Section 5 some results of numerical simulation for this latter mapping will be presented. Note the symmetry of this system: $y \to -y$; $\theta \to \theta + \pi$.

b. The standard map

For treating the separatrix mapping (3.3) analytically we introduce another approximate model[4] by linearizing the second equation (3.3) in y around one of resonant values of $y = y_r$ where $\lambda \cdot \ln y_r = 2\pi r$, and r is any integer. We get the map

$$\overline{I} = I + K \cdot \sin \theta; \qquad \overline{\theta} = \theta + \overline{I} \qquad (3.4)$$

which is called the standard map since it is the final reducing step for a number of particular problems in nonlinear dynamics[4]. The new momentum $I = (y_r - y)\lambda / y_r$, and the perturbation parameter:

$$K = - \frac{\lambda}{y_r} \qquad (3.5)$$

The standard map provides a local (in y) description for the previous model (3.3) under the condition: $|y_r - y_{r-1}| \ll y_r$, or $\lambda \gg 2\pi$. Note an additional symmetry of this map: $I \to I + 2\pi r$, which is not present in (3.3). It is just this symmetry that considerably simplifies the motion analysis since it makes the motion structure periodic in momentum I. Hence, instead of a phase cylinder for map (3.3) we have now a $2\pi \times 2\pi$ torus.

We, further, replace a discrete system (3.4) by the completely equivalent continuous one with Hamiltonian[4]

$$H(I, \theta, t) = \frac{I^2}{2} + K \cdot \sum_{r=-\infty}^{\infty} \cos(\theta - 2\pi r t) \qquad (3.6)$$

which has an infinite series of (integer) resonances $I = I_r = 2\pi r$. If we single out one of them, say, r = 0, and ignore (average out) all the others, we just come back to the pendulum whose motion we intended to study in this way. It is easy to see that leaving two more terms in series (3.6) (r=±1) we completely recover the original problem (2.1) with the parameters:

$$\omega_o^2 = K; \quad \Omega = 2\pi; \quad \lambda = \frac{2\pi}{\sqrt{K}}; \quad \varepsilon = 2 \qquad (3.7)$$

Yet, it is not a vicious circle but a spiral of cognition! In a more formal language it is called renormalization.

Now, let us mention, first of all, that the dynamics of a single nonlinear resonance can be described as a pendulum motion, or in the "pendulum approximation". As is shown in [4], this approximation is applicable under fairly broad conditions. Moreover, the original problem (2.1) relates to the dynamics of several (three) resonances and, hence, does include also the resonance interaction. Here, precisely, lies the importance of the Poincaré example and of the Poincaré problem.

Renormalized system (3.6) is not completely equivalent to the original one (2.1) in that the former has infinitely many resonances instead of three only for the latter. At the first glance, the problem becomes, thus, much more complicated, yet this is not the case. Just due to periodicity in I, the standard map, unlike the perturbed pendulum, has a sharp critical value of its parameter $|K| = K_{cr}$ which separates the bounded and unbounded variation of I. What is this critical value? First, we may just refer to the numerical simulation[4] which gives $K_{cr} = 0.989 \approx 1$ to the accuracy within a few percent. Using completely different approach, based on a combination of analytical as well as numerical procedures, Greene[10] has found $K_{cr} = 0.971635$. This latter result has been confirmed also in [11]. The accuracy of this value is open to criticism [12], yet, in any event, it is fairly close to the above numerical result.

The critical K value can be also estimated, in order of magnitude, from a simple resonance overlap criterion[4]

$$S = \frac{(\Delta \omega)_r}{\delta \omega_r} \approx \frac{4\sqrt{K}}{2\pi} \approx \frac{4\Omega_\phi}{2\pi} \sim 1 \qquad (3.8)$$

where Ω_ϕ is the frequency of small phase oscillation on a resonance, $(\Delta \omega)_r$ is the resonance width, and $\delta \omega_r$ is the spacing of resonances under consideration. Even though Eq. (3.8) gives the correct order it considerably overestimates $K_{cr} \sim 2.5$ because only integer resonances $(\omega_r = I_r = 2\pi r)$ are taken into account. Meanwhile, in higher approximations of perturbation theory the full set of resonances $(\omega_{rq} = 2\pi \frac{r}{q})$ does appear which obviously lowers K_{cr}. A partial consideration of those higher order resonances results in a better estimate[4]: $K_{cr} \approx 1.1$.

Below the threshold, that is for $|K| < 1$ (we neglect the above discrepancies in K_{cr}), the I variation is strictly bounded by the resonance width: $|\Delta I| \lesssim 4\sqrt{K}$. Above the threshold the motion is generally (depending on initial conditions) unlimited in I, and chaotic[4].

The random nature of such a motion will be discussed in Section 4. Now let us, first, turn back to separatrix mapping (3.3). From Eq. (3.5) we immediately see that the motion near separatrix is chaotic within the layer $|y| \lesssim \lambda$, or:

$$|w| \lesssim w_s = \lambda |\xi| = 4\pi\varepsilon\lambda^3 e^{-\pi\lambda/2} \qquad (3.9)$$

This relation resolves[4] the Poincaré problem as to the dimension of a homoclinic region. Thus, the whole homoclinic structure generated by the two branches of split separatrix is chaotic and occupies a layer whose width is about λ times the separatrix splitting. That layer is commonly termed as the stochastic layer.

The accuracy of estimate (3.9) is not as high as that of K_{cr}. It relates to the fact that a resonant value y_r enters Eq. (3.5). Due to the symmetry of standard map in respect to the line $I = \pi$, the maximal relative uncertainty in the position of layer border is equal approximately to π/λ (comp.[4]). Actual accuracy is somewhat higher as we shall see below.

c. Numerical evidence

The first numerical verification of estimate (3.9) was undertaken[4] using the standard map as a model. Indeed, we have seen above that the latter is essentially equivalent to the original system (2.1) with parameters (3.7). As to the other resonances in (3.6), their contribution is exponentially small according to (3.9). There is an additional complication with the standard map related to the fact that parameter $\varepsilon = 2$ is no longer small. On the other hand, numerical simulation is much simpler, of course, for a map than for a continuous system like (2.1). The first numerical experiments showed, however, that Eq. (3.2) is not exact for the map, and an additional factor has to be introduced:

$$\xi \to \xi R_h ; \qquad R_h \approx 2.15 \qquad (3.10)$$

Even though this factor can be calculated analytically as an effect of higher approximations of perturbation theory[4], its actual evaluation seems to be formidable and constitutes an unsolved problem. This shows also that the above assumed condition $\varepsilon \ll 1$ is, generally, essential for the validity of Eqs. (3.2) and (3.9). Taking into account the factor (3.10), we arrive at the expression

$$w_s = 64\pi^4 R_h \frac{e^{-\pi^2/\sqrt{K}}}{K^{3/2}} \qquad (3.11)$$

to be compared with numerical data. In a completely different approach this estimate has been confirmed in [13] except for the correction (3.10). The first comparison[4] revealed a satisfactory agreement within a fairly wide parameter range comprising about 13 orders of magnitude for w_s ($0.05 \le K < 1$).

New and more accurate data, obtained by Vecheslavov, are presented in Fig. 1 as the dependence of w_s on motion time (the number of map iterations) for both the outer (curve 1) and the inner (curve 2) parts of stochastic layer (K = 0.5). Note unusually big fluctuations which we are going to discuss below (see, especially, Section 5c). The values of w_s were calculated from the mean motion period T_m for a single trajectory in the layer, using the relation

$$w_s = 32 \cdot exp\,(1 - \sqrt{K \cdot T_m}) \qquad (3.12)$$

It is obtained via simple averaging of Eq. (2.3) in w assuming uniform distribution of a trajectory over the layer (see below). Eq. (3.11) gives in this case $w_s = .0329$. Thus, the accuracy of simple estimate (3.11) is about 20 percent for this not a very big $\lambda = 8.89$. To improve the agreement, a correction due to frequency shift (2.7) can be introduced as follows. In the present case of a map with infinitely many resonances (3.6) this correction can be shown to yield:

$$\sqrt{K} \to \sqrt{K} \cdot \left(1 - \frac{K}{24}\right) \qquad (3.13)$$

The correction at unstable equilibrium is responsible for a

change in period T_m in Eq. (3.12). As a result, the value of w_s, for a given measured period T_m, would increase by a factor of $\exp(T_m K^{3/2}/24) \approx 1.18$. This leads to $w_1 = .0320$ and $w_2 = .0303$ which are fairly close to the predicted value (3.11). Note that correction (3.13) does change, of course, the analytical expression (3.9) as well, yet it is already included in empirical factor (3.10).

A nice agreement achieved in this way is, however, accidental since another correction, due to inhomogeneous distribution inside the layer, needs to be introduced. An example of the equilibrium distribution of a single trajectory is given in Fig. 2 as obtained[14] by numerical simulation of separatrix map (3.3) for $\lambda = 9$. The equilibrium density was defined as the trajectory mean sojourn time for a given interval of w (or y). Note that the invariant measure for separatrix map $d\mu_{sx} \propto dw \propto dy$ is proportional also to the measure of original system (2.1) near separatrix: $d\mu \propto dH/\omega(H) \propto dw\, T(w)$, and T is time unit for the map.

Apart from big fluctuations the average density near layer edge is about half of that at the center. Averaging Eq. (2.3) with this density results in an additional correction factor in (3.12) of about 1.16, and makes the corrected values of w_s still bigger: $w_1 = .0371$; $w_2 = .0352$. The average of these two values now exceeds the theoretical prediction by about 10 percent.

This latter discrepancy relates to the marginal resonance inside the layer which "repells" the layer edge outwards (for detail see [4], Section 6.2), and which, by the way, depends on the neglected phase shift in (3.3). The center of this resonance is at $w_r = 32 \cdot \exp(-2\pi r/\lambda) \approx .0273$ ($r = 10$). Since its half-width is approximately $2w_s/\lambda$ it "expands" the layer up to $w_s' = .0347$ decreasing the remaining discrepancy down to 4 percent which is fairly low. Moreover, this uncertainty is already of the order of difference between the two layer parts which makes another problem to be understood. Apparently, the difference is also determined by the correction to Eq. (2.3) which can be shown to have the form:

$$\omega_o T(w) = L \cdot \left(1 - \frac{w}{8}\right) - \frac{|w|}{4} + O(Lw^2); \quad L = \ln\frac{32}{|w|} \quad (3.14)$$

Thus, the period T is longer for oscillation ($w < 0$). Yet, the derivative

$$\omega_o \frac{dT}{dw} \approx -\frac{1}{w} \cdot \left(1 + \frac{Lw}{8}\right) \quad (3.15)$$

is bigger for rotation. Hence (see Eq. (3.5)), the outer part of the layer is wider, the total difference being

$$\frac{\Delta w_s}{w_s} \approx \frac{Lw_s}{4} \approx .066 \quad (3.16)$$

Formally, this is close to numerical result: $\Delta w_s/w_s \approx 0.056$. However, the same correction (3.14) leads (after averaging over the layer, $w \to w_s/2$) to reduction of the numerical value by half. Unfortunately, big fluctuations, clearly seen in Fig. 1, preclude from any definite conclusion as to this latter discrepancy.

4. Intrinsic Randomness of Dynamical Motion

Let us briefly discuss the nature of motion in stochastic layer. It is certainly very complicated, irregular, and, at least, does surprisingly resemble a "true" random process. A fundamental question is whether one can, in principle, discern the former from the latter. According to the algorithmic theory of dynamical systems, the answer to this question is negative [3]. That is, so to say, dynamical (deterministic) motion may happen to be, and actually does so quite often, as random, in a sense, as a "true" random process.

The crucial feature of random dynamics is the exponential local instability of motion described by the metric entropy (see, e.g. [1])

$$h = \sum \Lambda_+ \geqslant \Lambda_m ; \quad \Lambda_+ > 0 \quad (4.1)$$

where Λ_m is the maximal of Lyapunov exponents Λ_i (see, e.g. [15]). The motion is exponentially unstable if and only if $\Lambda_m > 0$. Hence, it suffices to find out Λ_m only, which is given by the relation

$$\Lambda_m = \lim_{t \to \infty} \frac{\ln \rho(t)}{t} \quad (4.2)$$

Here ϱ is any separation of two close trajectories in linear approximation, that is vector $\vec{\varrho}(t)$ satisfies the equations of motion linearized about a given trajectory of the system. Considerable simplification in calculating just Λ_m relates to the fact that the initial vector $\vec{\varrho}(0)$ can be chosen arbitrarily, so that one does not need to know any eigenvectors of the linearized equations. For this and other reasons the quantity Λ_m serves as a convenient practical criterion to discern between chaotic and regular motions in numerical simulation (see, e.g. [16]). Note that due to dependence of the motion frequencies on initial conditions, a linear local instability takes place, as a rule, even for the regular motion [17] ($\varrho \propto t$). It also implies that only the conclusion $\Lambda_m > 0$ is unquestionable.

In the algorithmic theory [3] the random means unpredictable, or, to be more precise, the uncomputable. That definition appears to be in accord with our intuitive ideas of what the random is like. For to predict with a limited precision each next (in time) state of an exponentially unstable dynamical system, one needs to know the next digits of the irrational numbers representing the initial conditions of motion. That is, so to say, for prediction of a trajectory one needs to know this trajectory beforehand as encoded in the initial conditions. The crucial point is that for $\Lambda_m > 0$ the trajectory does vitally depend on arbitrarily diminutive details of initial conditions. In other words, such a trajectory as if exposes more and more deep strata of the motion phase space. For such a random trajectory could run for ever the phase space has to admit arbitrarily small difference in initial conditions which means the continuity of this space. It is, precisely, the ultimate origin of random motion of an unstable dynamical system in classical mechanics.

Apparently, the above picture does not hold in quantum mechanics which leads to a different kind of "chaos", if any, even in a classically random quantum system [12]. Since classical mechanics is only an approximation to the real world, and, moreover, not the best one, the classical random dynamics is but a limiting case which is never reached. The importance of this limiting case is in that it gives a pattern of the random to be compared to more realistic physical models.

Beside the quantum mechanics the computer simulation of classical dynamics is of especial value in the context of this lecture. Since any quantity in digital computer is essentially integer, the simulating dynamical space is never continuous but rather "quantized" in a sense, and the true randomness is impossible. This makes a serious problem still to be solved. Preliminary considerations [12] lead to the conclusion that computer simulation of classical chaotic dynamics is, nevertheless, possible within a finite (and relatively short) time interval, and with the help of some special computational tricks. Let us just mention that essentially the same situation takes place in quantum dynamics as well [12].

In any event, the algorithmic randomness does not imply that the chaotic motion is completely random. Generally, it may include a regular part as well. A good example is just the motion in a stochastic layer. The phase trajectories here are regular to the accuracy of layer width which is exponentially small. On the other hand, the transitions from oscillation to rotation and backwards are random as are successive values of the motion period.

5. On structure of the chaos border

The random nature of motion generally does not determine its statistical properties, nor even implies the relaxation to some definite equilibrium. The latter complication, related to a possible instability of a quasi-equilibrium, will not be discussed here (see, e.g. [18,19]). In "simple" dynamical problems under consideration, like pendulum (2.1), there always exists the single and stable equilibrium, not necessarily a simple one though (see Fig. 2). Then, positive entropy ($h \geqslant \Lambda_m > 0$) implies mixing, that is a correlation decay, and, hence, a relaxation to that equilibrium. However, the relaxation is not necessarily exponential as is still assumed sometimes.

a. Correlations

The statistical properties of chaotic motion essentially depend on the correlation, as is well known. Consider, first, the standard map (3.4). The "force" correlation, we shall need later on, is defined by

$$C_F(\tau) = \langle \sin \theta(t+\tau) \cdot \sin \theta(t) \rangle \qquad (5.1)$$

where averaging is performed either along a trajectory (in motion time t) or over an ergodic component of the motion.

For sufficiently large K, when regular component of the motion is negligible, this correlation is known to decay fairly fast [20], so that the sum

$$S_F = \sum_{\tau=1}^{\infty} C_F(\tau) \approx - \frac{J_2(|K|)}{2} + \frac{J_2^2(|K|)}{2} \qquad (5.2)$$

does certainly converge. The last expression, where $J_2(|K|)$ is the Bessel function, was calculated in [21]; it takes into account the first four terms of the series only.

The law of a long time correlation decay ($\tau \to \infty$) is actually unknown thus far. Some numerical evidence suggests that it may be like $C(\tau) \to A \cdot \exp(-B\sqrt{\tau})$ (comp. [22,23]). Particularly, the numerical data [20], related to the standard map with K = 7.5 and rescaled in the log-log plot, do fairly good fit this dependence with A = 1.14 and B = 1.37. On the other hand, in case of a regular component of motion present (for K = 2.1, for instance) a power-type decay of correlation is observed (see below). The latter may be compared to a similar behavior of the hard sphere gas [24].

b. Diffusion near the border

If correlation decay is sufficiently fast a simple statistical description of the chaotic motion is possible by means of a diffusion equation. In case of standard map it reads

$$\frac{\partial f(I,t)}{\partial t} = D \cdot \frac{\partial^2 f(I,t)}{\partial I^2} \qquad (5.3)$$

where the diffusion rate

$$D(K) = \lim_{t \to \infty} \frac{\langle (\Delta I)^2 \rangle}{2t} = \frac{K^2}{4} \cdot \left[1 + 4 S_F(K) \right] \qquad (5.4)$$

For large K the correlation correction $S_F \sim |K|^{-1/2}$ (5.2) vanishes, and the diffusion rate approaches its limiting, uncorrelated value $D^{\infty} = K^2/4$. In the opposite case $|K| \to 1$ the correlation dominates, and diffusion rate rapidly decreases [4]

$$D(K) \approx a \cdot (|K| - 1)^{\alpha} \qquad (5.5)$$

where $a \approx 1/5$, and $\alpha \approx 2.55$ according to numerical simulation. This implies $S_F \to -1/4$ as $|K| \to 1$.

For separatrix mapping (3.3) the diffusion becomes inhomogeneous since the dependence $D(|K|)$ turns into $D(|y|)$ according to Eq. (3.5). Generally, the diffusion equation includes an additional (drift) term. Indeed, the Fokker-Plank-Kolmogorov (FPK) equation can be always written in the form (see, e.g. [25]):

$$\frac{\partial f}{\partial t} = - \frac{\partial Q}{\partial y}; \quad Q = -D(y) \frac{\partial f}{\partial y} + U(y) f \qquad (5.6)$$

Here $Q(y,t)$ is the flux, and $U(y)$ is the drift velocity related to equilibrium distribution $f_0(y)$ by the expression

$$U(y) = \frac{d D(y)}{dy} + D(y) \frac{d}{dy} \ln f_0(y) \qquad (5.7)$$

Inspection of Fig. 2 shows that there are two regions within a stochastic layer where the drift can be neglected:

i) near the layer center where $f_0(y)$ = const exactly (variations of f_0 seen in Fig. 2 are due to fluctuations), and where $D(y) \approx D^{\infty} = 1/4$;

ii) near the layer border where $f_0(y) \approx$ const approximately only (see below), and where (see Eqs. (5.5) and (3.5)):

$$D(y) \approx a \cdot \left(1 - \frac{|y|}{\lambda} \right)^{\alpha} \qquad (5.8)$$

Generally, the dependence $U(y)$ is rather complicated. Since the border line is of a complicated shape, the y variable abo-

ve (as well as θ) is assumed to have been transformed in such a way as to "straighten out" this line $(|y_\ell| = \lambda)$.

In a model like (2.1) the diffusion spreads across the layer, and is obviously restricted by a finite layer width. Neglecting so far the slow diffusion (5.8) at the layer edges, it takes $t_r \sim \lambda^2$ iterations for a trajectory to get across the layer, or for a distribution function to relax. Since, however, Eq. (5.4) still holds a long time correlation does arise due to the boundary conditions. How simple the nature of that correlation may appear, it led to a paradox (or, rather, misunderstanding) [26-28] that the mixing precludes the diffusion instead of implying it. A formal reason for such a surprise conclusion is in that the mixing does provide existence of the limit in (5.4), while the paradox is a result of too literal understanding of this limit. It reminds us about an additional (besides the mixing) condition for the diffusion description of relaxation in a chaotic system to be applicable. Namely, there must exist two different time scales of the motion

$$t_c \ll t_r \qquad (5.9)$$

that of correlation decay (t_c) on which the limit (5.4) is asymptotical, and the other one of relaxation (t_r) on which the same limit is local. For example, the motion in a stochastic layer has $t_c \sim 1$, and $t_r \sim \lambda^2$, so that the condition (5.9) requires $\lambda \gg 1$.

The long time correlation within stochastic layer is of a primary importance in many-dimensional systems where the diffusion along the layer (the so-called Arnold diffusion [4]) does generally occur. For the latter diffusion were long-range, it has to be independent from the diffusion across the layer (due to different perturbation terms involved, for example) to get rid of that correlation.

Now, what would be impact of the slow diffusion (5.8) on the motion in stochastic layer? It turns out to be crucial if the exponent $\alpha > 2$. Assume the following diffusion equation near the layer border

$$\frac{\partial f}{\partial t} = \frac{\partial}{\partial x} x^\alpha \frac{\partial f}{\partial x} \qquad (5.10)$$

where we have introduced a new variable $x = 1 - y/\lambda$ $(y > 0)$, and rescaled t appropriately. First, let us try to find the eigenfunctions, that is to solve equation:

$$\frac{d}{dx} x^\alpha \frac{df_\varpi}{dx} + \varpi^2 f_\varpi = 0 \qquad (5.11)$$

It admits a solution via the cylindrical functions $Z_p(z)(\alpha \neq 2)$:

$$f_\varpi(x) = x^{\frac{1-\alpha}{2}} Z_p \left(\frac{2\varpi x^{1-\frac{\alpha}{2}}}{\alpha-2} \right); \quad p = \left(\frac{\alpha-1}{\alpha-2} \right)^2 \quad (5.12)$$

If $\alpha < 1$ the solution is regular at x = 0, and the relaxation is exponential. However, for $\alpha \geq 1$ the solution is generally singular. In particular, if $\alpha > 2$ the function

$$f_\varpi(x) \sim \frac{\cos \left(\frac{2\varpi}{\alpha-2} \cdot x^{1-\frac{\alpha}{2}} + \ell \right)}{x^{\alpha/4}}$$

grows and oscillates indefinitely as $x \to 0$ $(\ell \sim 1)$. If one would impose an artificial boundary condition at $x = x_1 \neq 0$, the eigenvalue $\varpi^2 \sim x_1^{\alpha-2} \to 0$ as $x_1 \to 0$. Hence, for the natural boundary at x = 0 no (regular) eigenfunctions do exist, and one would expect a nonexponential relaxation.

The general solution of this diffusion problem is not known. However, we may analyze a particular self-similar solution to Eq. (5.10) which, as is easily verified, reads:

$$\varphi_s' \equiv \frac{d\varphi(s)}{ds} = C \cdot s^{-\alpha} \cdot \exp \left(-\frac{1}{(\alpha-2)^2 s^{\alpha-2}} \right) \qquad (5.13)$$

Here C is an arbitrary constant, and $s = x \cdot t^{1/(\alpha-2)}$. At x = 0 the flux

$$Q(x,t) = -x^\alpha \frac{\partial \varphi}{\partial x} = -x^{\alpha-1} s \varphi_s' = \frac{C}{t^{\frac{\alpha-1}{\alpha-2}}} \cdot \exp \left(-(\alpha-2)^{-2} \cdot s^{2-\alpha} \right) \quad (5.14)$$

is always zero, while density $\varphi(s)$ may be non-zero (for $C < 0$). Due to self-similar nature of this solution the second bounda-

ry condition cannot be imposed at any fixed x (e.g., at the layer center, x = 1). However, asymptotically as $t \to \infty$ it doesn't matter since the diffusion mainly proceeds in an ever narrowing region at the layer edge. The size x_D of this region ($S \sim 1$) scales with t as $x_D \propto t^{-1/(\alpha - 2)}$, while for $S \to \infty$ the flux (5.14) becomes independent on x.

If initial density at the layer edge is less than that at equilibrium the relaxation corresponds to a negative (i.e. toward the edge) flux ($C > 0$), and to the boundary conditions:

$$\varphi(0,t) = 0; \quad \varphi(\infty,t) = \beta C \approx f_0 = 1; \quad \beta = \frac{\Gamma\left(\frac{\alpha-1}{\alpha-2}\right)}{(\alpha-2)^{\frac{\alpha}{\alpha-2}}} \quad (5.15)$$

where equilibrium distribution f_0 is assumed to be constant, and $\Gamma(z)$ is the gamma function. Asymptotically as $t \to \infty$, and except the diffusion region $\sim x_D$, the relaxation proceeds as follows

$$|\varphi(x,t) - \varphi(x,\infty)| \to \int_t^\infty |Q| \, dt = \frac{\alpha-2}{\beta \cdot t^{\frac{1}{\alpha-2}}} \quad (5.16)$$

In the opposite case a similar positive flux sets in ($C < 0$), and Eq. (5.16) remains unchanged. Thus, the slow diffusion ($\alpha > 2$) near the chaos border results in a power-type relaxation.

Since the time correlation of a pair of functions depends on the relaxation for one of them, we would expect, generally, the same power law (5.16) for the correlation as well. The latter may be faster though, if the relaxing function is close to equilibrium one near the border already from the beginning.

There is an interesting experiment on the behavior of electrons in a magnetic trap [29] which appears to confirm a power-type relaxation. The authors [29] observed a nonexponential dependence on time for the electron current $J(t) = -e\dot{N}$ out of the trap, due to a chaotic motion of electrons in inhomogeneous magnetic field, and did fit it by a double exponential function. On the other hand, the chaotic region of that

electron motion is known to always have the border [4]. If one rescales the data [29] in the log-log plot, as shown in Fig. 3, they perfectly fit, for sufficiently large time, the power dependence $\dot{N} \propto t^{-q}$ with exponent $q \approx 2.2$. This is to be compared to the flux (5.14): $Q \propto t^{-\frac{\alpha-1}{\alpha-2}}$, whence $\alpha \approx 2.83$. Remarkably, this value is not far away from that for the standard map ($\alpha \approx 2.55$, see (5.5)). It indicates some universal behavior near the chaos border. For further studies of this behavior the Poincaré recurrencies proved to be very useful [14].

c. Poincaré recurrencies

Consider separatrix map (3.3), and follow a single trajectory while it crosses successively the symmetry line y = 0. The motion time interval between two successive crossings we shall call the recurrence time τ. As motion proceeds the distribution of τ values tends to a limiting function $F(\tau)$ defined as the probability for a recurrence to occur later than τ. Obviously, F(1) = 1 (for the map), and generally $F(\tau) \to 0$ as $\tau \to \infty$. An exception from the latter is, for example, the asymptotic motion (2.5) along the unperturbed pendulum separatrix. Note that in case of the motion with discrete spectrum (quasiperiodic or almost periodic motions) $F(\tau) \equiv 0$ at any τ greater than some τ_r, while in chaotic motion $F(\tau) \neq 0$ for all τ. Poincaré recurrencies do not imply, thus, quasiperiodicity as is stated sometimes.

In stochastic layer motion the asymptotic behavior of $F(\tau)$ as $\tau \to \infty$ relates to the structure of the layer border. Such an approach was actually used in [30] where the power dependence

$$F(\tau) \sim \frac{1}{\tau^p}; \quad \tau \geqslant 1 \quad (5.17)$$

has been found with p = 1/2. As was pointed out in [14] it corresponds to the free homogeneous diffusion until the layer border is reached, that is for $\tau \lesssim \lambda^2$. Indeed, the function $F(\tau)$ can be found from the solution $g(y,t)$ of the diffusion equation with boundary conditions: $g(0,t) = g(\infty,t) = 0$, and

with initial condition: $g(y,0) = d\delta(y)/dy$. As is easy to see, the solution can be taken as derivative of the Gaussian function $g(y,t) = -\dfrac{d}{dy} G(y,t)$, where $G = 2 \cdot \exp(-y^2/t)/\sqrt{\pi t}$. Since

$$F(\tau) = \frac{\sqrt{\pi}}{2} \int_0^\infty g(y,\tau)dy = -\frac{\sqrt{\pi}}{2} \int_\tau^\infty q(0,\tau)d\tau \quad (5.18)$$

where $q = (1/4)\partial g/\partial y$ is the flux, and normalizing factor $\sqrt{\pi}/2$ is introduced to provide $F(1) = 1$, we get $F(\tau) = (\sqrt{\pi}/2) G(0,\tau) = \tau^{-1/2}$ and recover the result [30] (5.17).

At larger $\tau \gg \lambda^2$ the dependence $F(\tau)$ approximately remains of a power type but the exponent p changes; according to numerical data [14] the average p for various λ is $\langle p\rangle \approx 3/2$. In Fig. 4 an example of distribution $F(\tau)$ is given in the log-log scale [14]. A typical feature of this dependence is an apparently irregular variation of the logarithmic derivative $d\log F/d\log\tau \approx p$. The last part of the curve in Fig. 4 is unreliable due to a poor statistics (see numbers in the right lower corner of the figure). The variation does not depend on trajectory and, thus, characterizes the structure of the chaos border rather than fluctuations in motion.

Actually, it is not known if the observed dependence $F(\tau)$ does really relate to the layer border only. It may depend also on internal chaos borders encircling many islets of stability in the peripheral part of the layer (see Fig. 2). Assuming, nevertheless, that it is not the case we may try to interpret Poincaré recurrences, using, as above, the diffusion equation (5.10). Self-similar solution (5.13) cannot satisfy simultaneously both boundary conditions ($\varphi(0,t) = \varphi(\infty,t) = 0$) we need to apply Eq. (5.18). However, one can argue that the precise behavior of the solution at x = 0 is unimportant for the flux at $x \to \infty$. Then, we choose $\varphi(\infty,t) = 0$ ($C < 0$) and make use of the second expression (5.18) to get:

$$F(\tau) \propto \frac{1}{t^{\frac{1}{\alpha-2}}} \quad (5.19)$$

For the average observed value [14] $\langle p\rangle = 1.45$ the diffusion

parameter $\alpha = 2.69$ is comparable with previous values 2.55 and 2.83. Moreover, the change of the term $\lambda \cdot \ln|y|$ in map (3.3) for $\lambda^2/|y|$ did not alter p much [14]: p = 1.71 and $\alpha = 2.58$. Similar results have been also obtained by Shepelyansky with standard map for K = 2.1 and 5 when some islets of stability are present (in the latter case the relative stable area amounts to about 1.5 percent only [4]). At K = 2.1 p = 1.90; $\alpha = 2.53$, and for K = 5 p = 2.21; $\alpha = 2.45$. In spite of some dispersion in α values, which is partly due to empirical uncertainties (as p variation, see Fig. 4), they are surprisingly close in different models that again suggests some universal behavior at the chaos border (see below, Section 5d).

On the other hand, for K = 7, when the regular component is negligible, if any, the recurrencies, as expected, are perfectly exponential over 6 orders of magnitude:

$$F(\tau) = e^{-\frac{\tau - 1}{\tau_r}} \quad (5.20)$$

with $\tau_r = 1.73$. Note that comparison of this value with the theoretical prediction based upon diffusion equation (5.3) is now precluded due to violation of condition (5.9): $t_c \sim \tau_r \sim 1$.

For all apparent success of the above interpretation of Poincaré recurrences one serious difficulty should be mentioned: the relation (5.19) contradicts with a simple and almost obvious estimate [14] based upon ergodicity of motion. Namely, the measure of the region where trajectory spends its recurrence time τ would be of the order $\tau F(\tau) \sim x_D$ (see Section 5b, and we assumed the total number of recurrences $N \sim t$, the total motion time [14]). The question is what's that region? According to the above picture of motion near the border it seems to be the diffusion region $x_D \propto \tau^{-\frac{1}{\alpha-2}}$, whence $F(\tau) \sim 1/t^{\frac{1}{\alpha-2}+1}$ in contradiction with (5.19). Even if the latter expression were exact solution to diffusion equation (5.10) it would be very difficult to match this solution to numerical data. An alternative approach will be discussed at the end of the next Section.

d. Scaling

As was mentioned above there are numerical indications suggesting some universal behavior near the chaos border in the phase space. Now we are going to consider a theoretical model for this alleged universality. That the resonance structure determining transition to chaos is hierarchic has been known already since quite long ago (see, e.g. [31,4]). Yet, only in the pioneering work due to Greene [10] that structure has been exploited to evaluate a critical perturbation for the standard map which, at least, is very close to the true one (see [12] and Section 3b above for discussion). Hierarchic and scaling behavior at the transition to chaos was further studied extensively in many papers (see, e.g. [11,13] and references therein). A distinctive feature of our problem (see also [35]) is in that the perturbation strength here is not a parameter, as for standard map, but rather a function of dynamical variables (mainly, momentum y for separatrix map (3.3)). This leads just to a chaos border in the phase space rather than to a critical perturbation strength.

Assume the following scaling hypothesis: near the chaos border any two of dynamical variables (v, u) are interrelated by a power dependence:

$$v \propto u^{P_{uv}} \qquad (5.21)$$

where P_{uv} is scaling parameter, and $P_{uv} \cdot P_{vu} = 1$. Choosing one variable (u) as the fundamental scaling unit we have

$$v \propto u^{P_v} \qquad (5.22)$$

Such a scaling hypothesis is essentially identical to that in the fluctuation theory of phase transitions [32] which leads to some similarity of these two problems. However, important distinctions should not be missed. The scaling in phase transitions is continuous and essentially statistical (fluctuation scaling), while in our problem scaling is discrete (see below), and does relate to both chaotic as well as purely regular components of motion on both sides of the chaos border.

What makes the two problems similar is a crucial impact of an infinite sequence of scales (continuous or discrete) upon the behavior at transition.

Transform (x, θ) variables in such a way as to provide near the border: $x \propto |\omega(x) - \omega_\ell|$, $2\pi\omega(x)$ being the motion frequency of system (3.3) under consideration, and $\omega_\ell = \omega(0)$ the frequency at the border $x = 0$. Hence: $p_x = p_\omega$, or, choosing ($\omega - \omega_\ell$) as the fundamental scaling unit ($p_\omega \equiv 1$), $p_x = 1$. Note that in original variables (before the transformation) the exponent p_x would depend on θ (see [11]).

The measure of chaotic component $\mu \propto x$, since at the border the resonances are just about to overlap in all scales (comp. Fig. 2), whence $p_\mu = 1$.

To proceed furher we need to relate these scales to that of time. It can be done via the overlap parameter s (3.8). The width $(\Delta\omega)_q$ of a high order resonance $\omega_q = r/q$ depends on its phase oscillation frequency Ω_q as (see, e.g. [4,5]): $q(\Delta\omega)_q \sim \Omega_q$, while the resonance spacing $\delta\omega_q \sim q^{-2}$. The latter follows from the total number of resonances, within a given interval of ω, which is proportional to q^2. In a more formal way it is also implied from the best approximation of a given irrational number (ω_ℓ in our case) by the convergents of the continued fraction representation (see, e.g. [33]):

$$\left| \omega_\ell - \frac{r}{q} \right| \sim \frac{C(\omega_\ell)}{q^2} \qquad (5.23)$$

Hence, at the chaos border

$$s_q = \frac{(\Delta\omega)_q}{\delta\omega_q} \sim q^2 (\Delta\omega)_q \sim q\,\Omega_q \sim 1 \qquad (5.24)$$

The overlap parameter s_q is related to the Greene residue [10] : $R_q \sim s_q^2$. For standard map with $|K| = K_{cr}$ which corresponds to the chaos border in map (3.3), $R_q \to 1/4$ as $q \to \infty$ [10] in accordance with estimate (5.24).

Suppose that a given scale is essentially determined by some resonance ω_q. Then, the associated time scale would be $T_q \sim \Omega_q^{-1}$, and $(\Delta\omega)_q \propto |\omega_q - \omega_\ell|$. Whence, $p_T =$

$p_q = -1/2$. The scaling for diffusion rate near the border is, hence $D \propto (\Delta\omega)_q^2/T_q \propto x^2/T \propto x^{2.5}$, and the diffusion parameter $\alpha = 5/2$ which is close to various numerical values given above ($2.45 \leq \alpha \leq 2.83$). With $\alpha = 5/2$ both the relaxation as well as correlation go asymptotically as t^{-2}. This law, being nonexponential, does, at least, imply a final diffusion rate according to (5.2) and (5.4). It results, however, in big fluctuations near the chaos border (see, e.g., Fig. 1). Earlier, such fluctuations have been observed, and qualitatively explained [4], in the Arnold diffusion.

Since resonance width $(\Delta\omega)_q \propto V_q^{1/2}$, where V_q is corresponding Fourier amplitude of the limiting perturbation in Hamiltonian (see below), the scaling (5.24) implies $V_q \propto q^{-4}$, that is the perturbation has two continuous derivatives only. This is precisely the critical smoothness of perturbation for the map [34,4]. It means the following. If initial perturbation $V^\circ(\theta)$ is analytic function, its Fourier amplitudes, as is well known, fall off exponentially, like $V_q^\circ \propto exp(-\sigma^\circ q)$, for example. However, as we proceed to higher approximations the amplitudes grow, or parameter σ decreases [36]: $\sigma^\circ \to \sigma(K)$. At critical perturbation the dependence V_q on q becomes, as everything else, of a power-type, that is $\sigma(K_{cr}) = 0$ (see [10]). On the other hand, as is also known [34], the initial perturbation needs not be analytic for a chaos border to exist, instead it suffices for $V^\circ(\theta)$ to be only smooth, that is $V_q \propto q^{-p_o}$ provided $p_o > p_{cr}$. Otherwise, the motion is chaotic for any non-zero perturbation strength.

As was mentioned above the scaling near the chaos border is discrete. It means that there exists a denumerable sequence of principal scales which is determined by a corresponding sequence of resonances $\omega_{q_n} = r_n/q_n$ converging to the border: $r_n/q_n \to \omega_B$ as $q_n \to \infty$. The resonance sequence depends on arithmetical properties of irrational ω_B, for example, on its representation as a continued fraction: $\{\omega_B\} = [\ell_1, \ell_2, \ldots, \ell_n, \ldots]$ where $\ell_i \geq 1$ are integers, and curly brackets denote the fractional part. According to Greene's conjecture [10] ω_B is the "golden mean", i.e. $\{\omega_B\} = g_1 = [1, 1, \ldots, 1, \ldots] = (\sqrt{5}-1)/2 \approx .618$.

It is not known whether this is true for the standard map but generally it does not hold [12,35]. A much weaker hypothesis that ω_B has a "golden tail", i.e. $\{\omega_B\} = [\ell_1, \ldots, \ell_n, 1, \ldots, 1, \ldots]$, seems plausible.

In case of the chaos border the main problem is to match the arithmetic of ω_B to the critical value of K which depends on x. On the golden tail the estimate (5.23) becomes exact with $C \to 1/\sqrt{5} \approx 0.45$, the biggest one for irrationals of the type $g_m = [m, \ldots, m, \ldots]$. Following Greene [10] we assume the principal scales to relate to the "golden" convergents q_n. Then, the scaling factor $\sigma_q \equiv q_{n+1}/q_n \to 1 + g_1$. Since the sign of successive differences $(\omega_B - r_n/q_n)$ alternates the actual scaling factor on the chaotic side from the border is $\sigma_q^2 (= \sigma_T^2)$. Hence, one would expect a variation of the border structure, the period, in log$t$ scale, being $\ell_t = 2 \cdot log\,\sigma_T \approx 0.42$. This qualitatively explains the observed variations of exponent p for Poincaré recurrences (see Fig. 4). However, the above value of ℓ_t seems too small as compared to numerical data [14] ($\ell_t \approx 1 \div 1.5$). The latter show also a rather irregular variation.

On the other hand, for almost any irrational ω_B the average $\langle \ell_t \rangle = \pi^2/6 \cdot \ell n\,2 \cdot \ell n\,10 \approx 1.03$ with big fluctuations towards larger ℓ_t (see, e.g. [2,33]). This seems to be more in conformity with numerical data. Yet, it does not necessarily refute the golden tail hypothesis. Instead, it is quite possible that, generally, the tail begins too far to be seen in numerical simulation unless the system parameters (λ in our case) are specially adjusted.

The principal resonances, which determine the above scaling factor, account also for the shape of the border line. A crude estimate for this shape can be evaluated as follows. On each scale the resonance strip (around a "queue" of its fixed points) approximately follows a nearby resonance separatrix of a larger scale. A relative slope of separatrix to its resonance strip scales as $\gamma_q \propto (\Delta\omega)_q/q^{-1} \propto q^{-1}$ (see Eq. (5.24)). Hence, the sum $\Gamma \sim \sum_q \gamma_q$ estimates the "absolute" (in original variables) slope of the border line.

Since the proportionality factors for each γ_q are varying with θ, and, particularly, change sign, this sum diverges at the very special θ only, which, however, may form a dense set. Near a singular point (say, $\theta = 0$) the border shape is roughly determined by the sum

$$\Gamma(\theta) \sim \sum_q \frac{1}{q} \cos\left(\frac{q\theta}{2}\right) \sim \ln\frac{1}{\theta}$$

Since the scaling exponents depend on θ, this singularity is, generally, of a power-type as has been found in [37],[11]. Yet, for some points one might expect the logarithmic singularity as well.

Finally, let us estimate the contribution to Poincaré recurrences from internal chaos borders of resonance stochastic layers. That there are many such layers within the main layer is immediately seen in Fig. 2 from a low equilibrium density near the border. It also follows from the limiting value of Greene residue $R = 1/4$ which means that the resonance centers near the border are not destroyed.

Let the time scale of a given resonance be T_q. Then the mean sojourn time in its region of measure $\mu_q \propto x_q$ is, due to ergodicity, $N_q T_q / t \propto x_q$ where N_q is the number of entries into this region, and t is the total motion time. Assume the universal distribution of Poincaré recurrences $F(\tau) \propto \tau^{-p}$ with some, unknown so far, p. Particularly, this implies the probability $F_q \propto (T_q/\tau)^p \propto (q/\tau)^p$ $(\tau \gtrsim q)$ for any internal chaos border of a resonance stochastic layer. Then, the contribution to Poincaré recurrences in the main layer from a particular resonance would be

$$F^{(q)} \propto \frac{N_q F_q}{N} \propto \frac{x_q \cdot q^{p-1}}{\tau^p} \cdot \frac{t}{N} \propto \frac{q^{p-3}}{\tau^p} \quad (5.25)$$

where $N \propto t$ is the total number of recurrences. Now we need to sum up the contributions of all undestroyed resonances which retain their stochastic layers. The number of those resonances can be estimated as follows. Define the border zone $x_z(q)$ as $\sigma(x_z) \cdot q \sim 1$ where $\sigma(x)$ is the exponential factor of the perturbation Fourier amplitudes introduced above. Assuming the linear dependence $\sigma(x) \propto x$ near the border we arrive at the scaling $x_z \propto q^{-1}$ for the border zone size. The latter implies that for a given q just one resonance gets into this zone, so we are to merely sum up contribution (5.25) over q:

$$F' \sim \sum_q^{\tilde{\tau}} F^{(q)} \propto \frac{1}{(p-2)\tau^2}, \, p > 2; \quad F' \propto \frac{\ln\tilde{\tau}}{\tau^2}, \, p = 2$$

From universality $F'(\tau) \sim F(\tau)$, and $p = 2$. First of all, this would imply that the main contribution to Poincaré recurrences were not due to the diffusion near the main layer border but from a labyrinth of infinite hierarchies of internal chaos borders where trajectory spends the most of its recurrence time. This resolves the difficulty with ergodicity discussed above. However, if confirmed, it would also mean that near the chaos border the above scaling hypothesis holds only approximately, to logarithmic accuracy. This also would change the behavior of both relaxation as well as correlation near the chaos border as compared to estimates in Section 5b based upon the diffusion equation (5.10).

Certainly, the problem of chaos border structure, whose particular case is a still unsolved part of the Poincaré homoclinic problem, needs and deserves further studies.

Acknowledgements

References

1. V.I.Arnold and A.Avez, _Ergodic Problems of Classical Mechanics,_ Benjamin (1968).

2. I.P.Kornfeld, Ya.G.Sinai, S.V.Fomin, _Ergodic Theory,_ Nauka, 1980 (in Russian).

3. V.M.Alekseev and M.V.Yakobson, Physics Reports, 75, 287, (1981).

4. B.V.Chirikov, Physics Reports, 52, 263 (1979).

5. A.J.Lichtenberg and M.A.Lieberman, _Regular and Stochastic Motion,_ Springer-Verlag (1982).

6. H.Poincaré, _Les méthodes nouvelles de la méchanique céleste._ Vol. II (1893), Sections 225-232; Vol. III (1899), Section 401.

7. N.N.Bogoliubov and Yu.A.Mitropolsky, _Asymptotic Methods in the Theory of Nonlinear Oscillations,_ Hindustan Publ. Corp., Dehli, 1961.

8. V.K.Melnikov, Dokl. Akad. Nauk SSSR, 144, 747 (1962) (in Russian).

9. L.P.Shilnikov, Mat. sbornik, 77, 461 (1968) (in Russian).

10. J.M.Greene, J. Math. Phys. 20, 1183 (1979).

11. L.P.Kadanoff, Phys. Rev. Lett. 47, 1641 (1981); S.J.Shenker and L.P.Kadanoff, J. Stat. Phys., 27, 631 (1982).

12. B.V.Chirikov, F.M.Izrailev, D.L.Shepelyansky, in _Soviet Scientific Reviews,_ Section C, Vol. 2 (1981), p. 209.

13. D.F.Escande, _Large-Scale Stochasticity in Hamiltonian Systems_, Intern. Conf. on Plasma Physics, Göteborg (1982).

14. B.V.Chirikov, D.L.Shepelyansky, _Statistics of the Poincaré Recurrencies and the Structure of Stochastic Layer of a Nonlinear Resonance,_ Preprint 81-69, Institute of Nuclear Physics, Novosibirsk (1981) (in Russian).

15. Ya.B.Pesin, Usp. mat. nauk, 32, No 4, 55 (1977) (in Russian).

16. J.Ford, S.D.Stoddard and J.S.Turner, Prog. Theor. Phys. 50, 1547 (1973).

17. G.Casati, B.V.Chirikov and J.Ford, Phys. Lett. 77A, 91 (1980).

18. P.Glansdorff and Prigogine, _Thermodynamic Theory of Structure, Stability and Fluctuations,_ Wiley, New York (1971).

19. H.Haken, _Synergetics,_ Berlin (1978).

20. C.Grebogi and A.N.Kaufman, Phys. Rev., A24, 2829 (1981).

21. A.B.Rechester and R.B.White, Phys. Rev. Lett., 44, 1586 (1980); A.B.Rechester, M.N.Rosenbluth and R.B.White, Phys. Rev., A23, 2664 (1981).

22. L.A.Bunimovich, Ya.G.Sinai, Comm. Math. Phys., 78, 479 (1981).

23. G.Casati, G.Comparin and I.Guarneri, Phys. Rev. A26, No 1 (1982).

24. B.Alder, T.Wainwright, Phys. Rev., A1, 18 (1970).

25. E.M.Lifshits, L.P.Pitaevsky, _Physical Kinetics,_ Nauka (1979) (in Russian).

26. J.L.Lebowitz, in _Statistical Mechanics, new concepts, new problems, new applications,_ Univ. of Chicago Press (1972).

27. R.Balescu, _Equilibrium and Nonequilibrium Statistical Mechanics,_ Wiley, New York (1975), Appendix.

28. G.E.Norman, L.S.Polak, Dokl. Akad. Nauk SSSR, 263, 337 (1982) (in Russian).

29. D.Bora, P.I.John, Y.C.Saxena and R.K.Varma, Plasma Physics, 22, 653 (1980).

30. S.R.Channon and J.L.Lebowitz, Ann. N.Y. Acad. Sci., 357, 108 (1980).

31. J.M.Greene, J. Math. Phys., 9, 760 (1968).

32. A.Z.Patashinskii and V.L.Pokrovskii, Fluctuation Theory of Phase Transitions, Pergamon (1979).

33. A.Ya.Khinchin, Continued Fractions, Fizmatgiz, Moscow
    (1961) (in Russian).

34. J.Moser, Stable and Random Motions in Dynamical Systems,
    Princeton Univ. Press (1973).

35. J.M.Greene, in Nonlinear Dynamics and the Beam-Beam Inter-
    action, A.I.P. Conf. Proc., No 57 (1979), p. 257.

36. V.I.Arnold, Usp. mat. nauk, 18, No 6, 91 (1963) (in Russi-
    an).

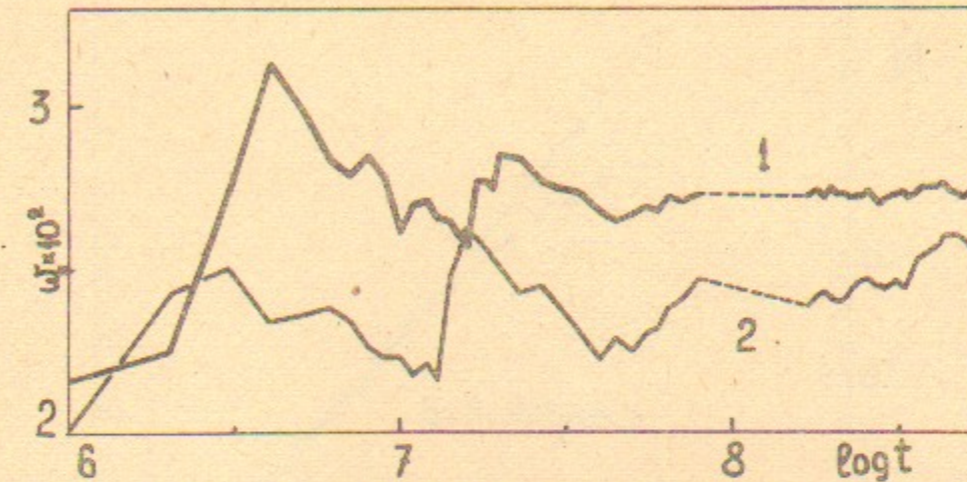37. J.M.Greene and I.Percival, Physica 3D, 530 (1981).

Fig. 1. The half-width of stochastic layer of an integer re-
sonance in standard map vs. motion time (number of
iterations): outer part of the layer (1); inner part
(2); K = 0.5.
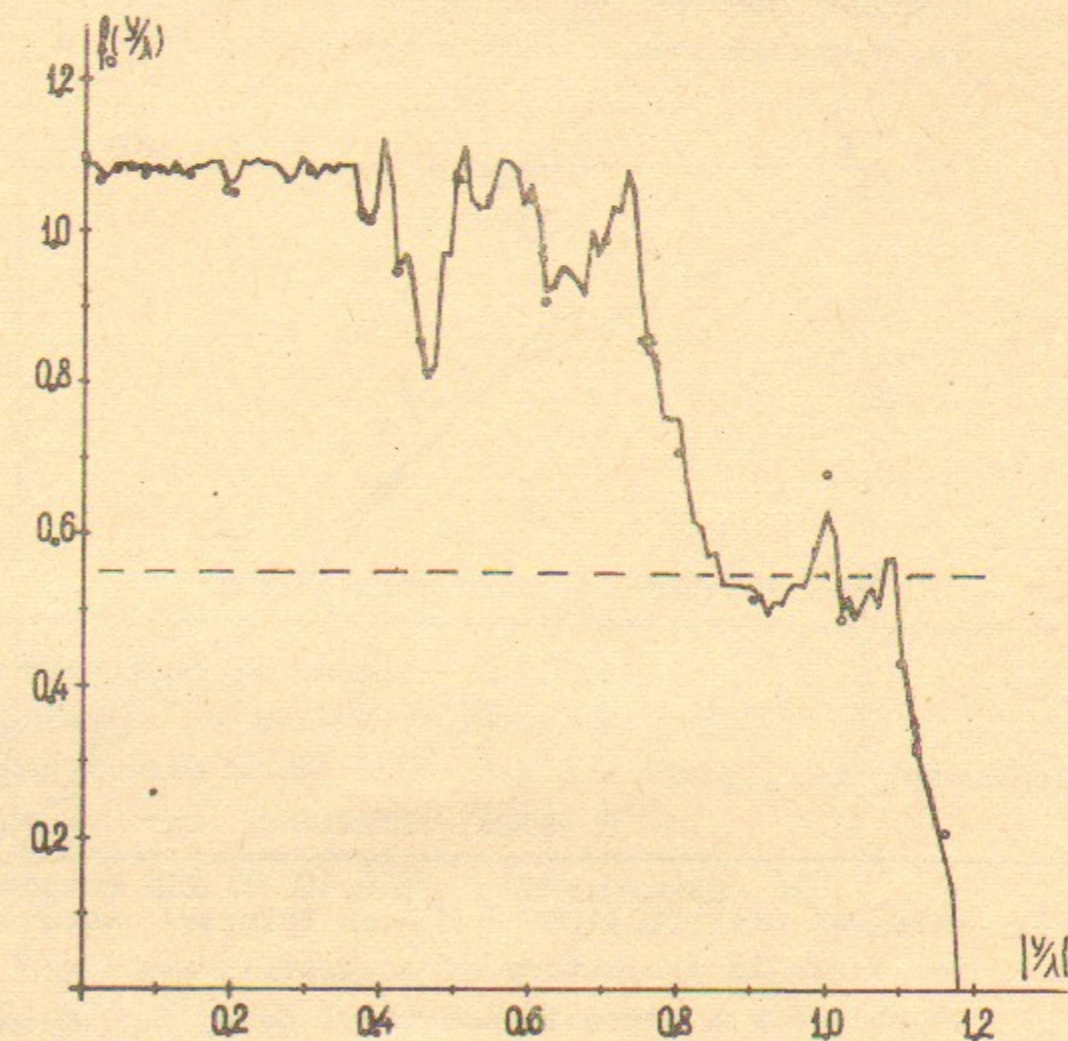
Fig. 2. Equilibrium distribution of a single trajectory in
stochastic layer after separatrix map [14] : $t = 10^7$
(broken line); $t = 4 \times 10^6$ (circles); $\lambda = 9$. Dashed
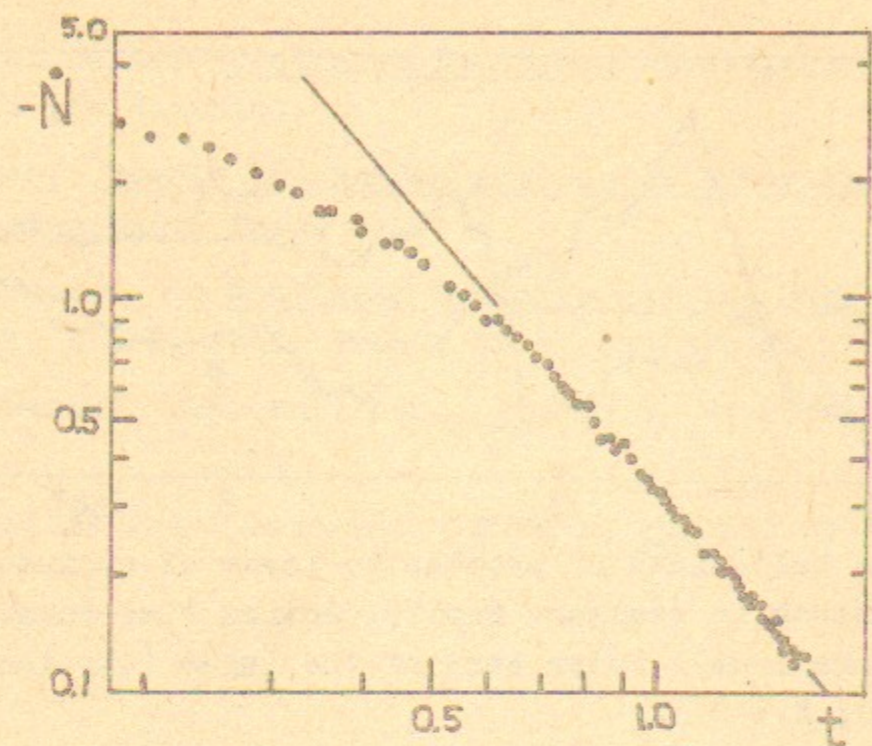line indicates the mean density near layer edge.

Fig. 3. Electron current out of magnetic trap (arbitrary units) vs. time (in msec)[29]. Straight line: $\dot{N} \propto t^{-2.2}$.
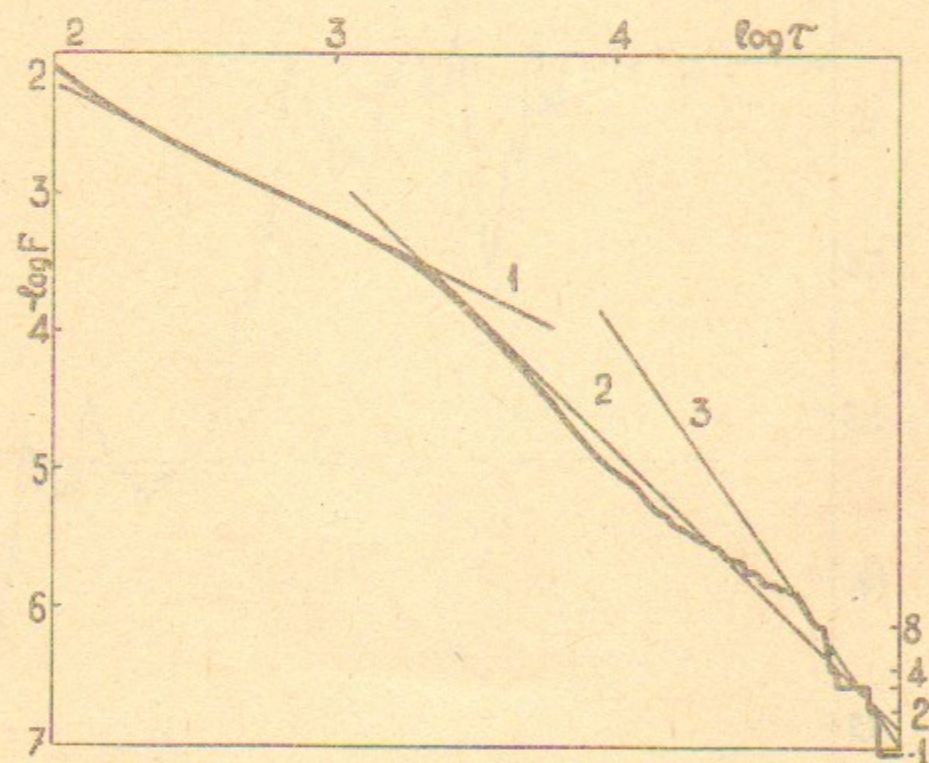

Fig. 4. Integral distribution $F(\tau)$ of Poincaré recurrences for a single trajectory of separatrix map (10^8 iterations): curve presents numerical data [14]; straight lines are: $F(\tau) \propto \tau^{-p}$ with p as indicated; absolute numbers of recurrences for large τ are given in the right lower corner; log = decimal logarithm.

Б.В.Чириков

ХАОТИЧЕСКАЯ ДИНАМИКА ГАМИЛЬТОНОВЫХ СИСТЕМ
С РАЗДЕЛЕННЫМ ФАЗОВЫМ ПРОСТРАНСТВОМ